INFLUENCE OF IMPACT ANGLE AND HUMIDITY ON TB11 VIRTUAL CRASH TESTS FOR SP-05/2 ROAD SAFETY BARRIER

DANIEL B. NYCZ[1]

Jan Grodek State Vocational Academy in Sanok

Summary

The paper presents a numerical study on the effect of selected factors, i.e. the impact angle and the dry/wet surface of roads and shoulders on the course of the TB11 virtual crash test. The testing is conducted for a N2-W4-A class barrier in a horizontal concave arc of 150 m radius, hit by a Geo Metro vehicle at an angle of 20°. The overlay is applied to approve the standard criteria, installed with screw connectors with rectangular rubber pads, fixed in the free holes of the guide. The numerical calculations were conducted in LS-Dyna environment, using a Geo Metro vehicle model, taken from the NCAC website and appropriately modified. The analysis included quantitative and qualitative crash test parameters, as per PN-EN 1317-1:2010 and PN-EN 1317-2:2010 standards. The designed composite-foam overlay allowed to adopt virtual crash tests for a standard-specific impact angle, under dry and wet conditions. The influence of the impact angle on the course of the crash test is complex. Increasing the angle to 30° can lead to unfulfilling the condition of redirecting the vehicle onto the road.

Keywords: TB11 virtual crash test, barrier in horizontal concave arc, composite-foam overlay, impact angle, humidity

1. Introduction

Modelling and numerical calculations for road crash tests are the subject of a number of publications. Their scope discusses several containment systems, e.g. steel [1, 6, 7, 9, 13, 19, 20, 22, 23] or concrete [3÷5, 10] guard barriers. Vehicle models are taken from the National Crash Analysis Center (NCAC), USA [29].

---

[1] Jan Grodek State Vocational Academy in Sanok, Institute of Technology, ul. Reymonta 6, 38-500 Sanok, Poland; e-mail: daniel.nycz@interia.pl

For steel barriers, in most cases, the analysis is conducted for straight barriers of varying containment levels, for example in papers [6, 7, 23] a H1 containment level (TB11, TB42) barrier is discussed and paper [15] discusses a N2 containment level (TB11, TB32) [25, 26] barrier.

Reference [19] presents the results of crash test simulations using the LS-Dyna system, being an impact of a light vehicle with a barrier in a horizontal concave arc of approx. 12 m radius and a W-type guiderail. The simplified vehicle model was taken from the NCAC library [29]. Steel material model was adopted as Ref. [1]. C150 post were mounted in concrete cylinders. The impact velocities were 40, 60 and 80 km/h. In all cases, the car hit the barrier at approximately 0° angle and slide along the barrier, without suffering major damage, and subsequently was correctly recovered from the interaction with the barrier. The aim of the testing was to compare the crash intensity using Acceleration Severity Index (ASI).

The analysis of the effect of the impact of Geo Metro vehicle into a concrete barrier in a horizontal arc of respectively a 50, 100 and 200 m radius and the direction of movement of the approaching vehicle was carried out in [3]. Based on these results, it was found that the most dangerous case is the collision of a vehicle with a barrier of a 50m radius, when the vehicle leaves the internal arc. Furthermore, it was found that that for this type of collisions the most dangerous are large impact angels of car onto the barrier.

In Refs. [6, 7], the authors carried out the modelling and simulation of TB11 and TB42 crash tests for barriers of H1 containment level. Vehicle models were taken from the NCAC public library [29]. They underwent some modifications. The straight barrier was modelled using shell elements, treating the guide as a continuous beam (without connectors). The authors investigated the effect of four structural changes to the road barrier: 1) introduction of tension belt, 2) introduction of roller guide, 3) introduction of rope at the top of the guide, 4) introduction of rope at the bottom of the guide. The virtual tests were compared to real crash tests. The analysis took into consideration only the ASI and THIV parameters for TB11 test, as well as working width for TB42 test.

Numerical calculations on the influence of the impact angle of the Geo Metro vehicle to the concrete road barrier were performed in Ref. [5]. The movement and vehicle deformations were presented, corresponding to angles of 10°, 20°, 30°, 40° respectively. The numerical model for the vehicle was taken from the NCAC [29] library. The subsequent paper [4] developed numerical modelling and simulations of TB11 and TB32 crash tests furthermore, taking into account fixed or movable segments of concrete road barriers. The results include the behavior and deformation of vehicles and an ASI index.

2. Tested System and Crash Tests under Scope of Analysis

The subject of research is a SP-05/2 road barrier of the N2-W4-A class, manufactured by Stalprodukt SA company, located in Bochnia [28]. The barrier consists of sections (a total length of 4.30 m each) of B-type guiderail, Sigma posts of 1.9 m length, and trapezoidal brackets and rectangular pads. All barrier elements are made of S235JR steel and were subjected to galvanizing process. M16 screws of the 4.6 class were used as connectors for the SP-05/2 system [27, 28].

According to Refs. [25, 26], the condition for the acceptance of the N2 containment class is to meet the crash analysis criteria for TB11 and TB32 tests (TB11: a vehicle of mass of 900 kg and a velocity of 100 km/h, an impact angle of 20°; TB32: a vehicle of mass of 1500 kg and a velocity of 110 km/h, an impact angle of 20°). Partial results of crash tests for SP-05/2 system were provided by the manufacturer [28].

Crash tests for the acceptance of containment systems are carried out on straight barrier sections, as defined in [25, 26]. In Refs. [16, 18, 21], based on TB11 and TB32 virtual crash tests, it was proven that a SP-05/2 system in arc of 150 m radius does not meet all the acceptance criteria for barriers in accordance with [25, 26]. The radius of 150 m is the smallest curvature radius of curved outside barriers of GP roads.

For the standard-specific criteria [25, 26] on road curves to be met by the SP-05/2 system, a foam-composite overlay of code CFR2 was designed [15, 16, 17, 21]. The CFR2 overlay solution is original and protected by a patent application [15].

The cross-section of CFR2 overlay was matched to a B-type road barrier guiderail. The total length of the overlay segment is 4.70 m with the effective length of 4.00 m. The overlay consists of a GFRP composite front and rear layers and foam fill. Polimal 104S polyester resin was used as the matrix for the composite layers. To reinforce the composite laminas, STR600 [0/90] balanced glass fabric with straight strand was used, as well as CSM450 glass mat . PUR S-42 polyurethane foam was used (fig. 1, 2).

The overlay segments are mounted in the free holes of the SP-05/2 system B-type guiderail, using M16x80 screws of class 8.8, via rectangular EPDM 70°ShA rubber pads and A-type rectangular steel pads, as specified in the Stalprodukt catalogue. Full description of the CFR2 overlay can be found in Refs. [15, 16, 17, 21].
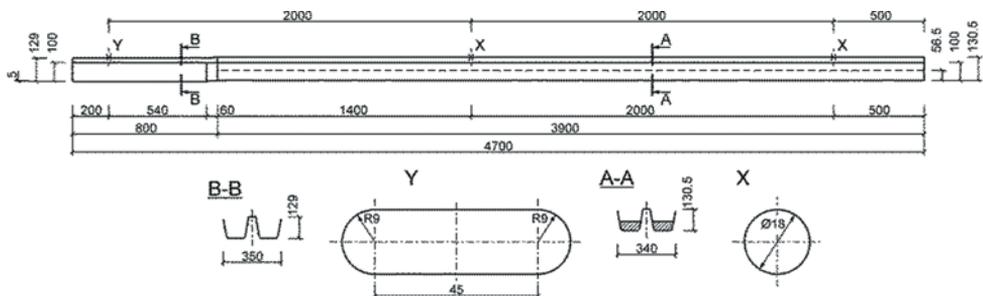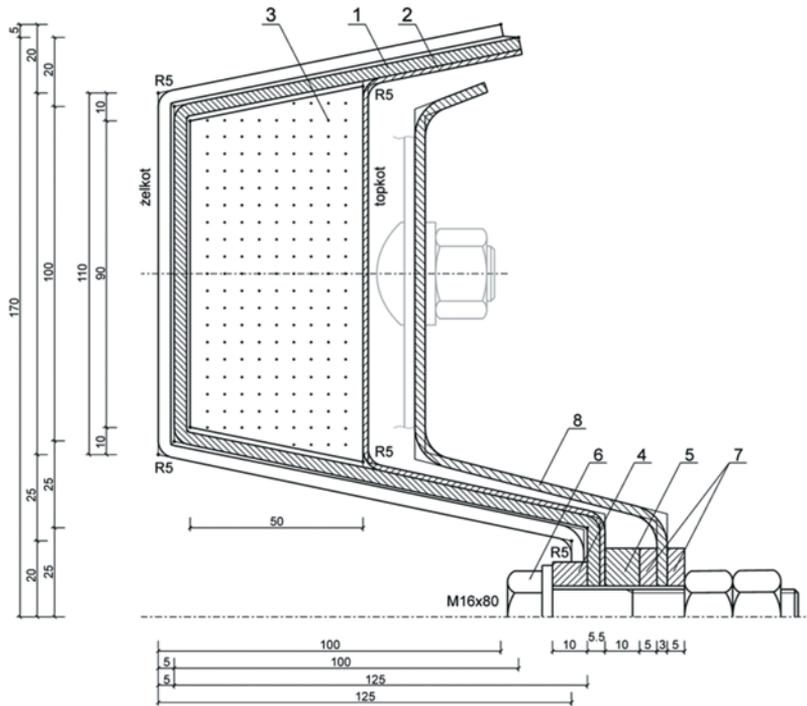

Fig. 1. Segment of CFR2 overlay [15-17]

Fig. 2. Cross-section of CFR2 overlay in X-axis joint: 1 – front laminate; 2 – rear laminate; 3 – polyurethane foam; 4 – front rubber pad; 5 – rear rubber pad; 6 – steel screw; 7 – rectangular A-type pad; 8 – B-type guide bar [15-17]

3. Numerical Models for Tested Settings

The virtual crash tests used a Geo Metro vehicle model developed by the NCAC. [29] It contains more than 33 000 of finite elements (over 35 000 nodes).

Based on the preliminary results of crash tests (e.g. frontal impact and a 20° angle impact of a vehicle with a rigid wall), it was found that modifications to the vehicle model are required: e.g. changing the model describing the work of tires, adjustments to the suspension model, including dynamic relaxation (gravity) before starting the vehicle-barrier impact process, correcting the contact model options and control cards.

The tested sections of a SP-05/2 barrier (straight and arc) were meshed using four-node shell finite elements in the Belytscho-Tsay formulation, with reduced integration points in the element plane (ELFORM_2 formulation according to Refs. [11, 12]). The soil, in which SIGMA posts were seated, was reflected using cylinders of 1.00 m radius and 1.30 m depth, meshed with solid elements of HEX8 and PENTA6 topologies, with the ELFORM_1 formulation assigned (solid elements with constant stress), [11, 12]. The composite elements

of the CFR2 overlay were meshed using four-node shell elements in the Belytscho-Tsay formulation, with reduced integration in the element plane (ELFORM_2) and one point of integration for each lamina [11, 12]. The polyurethane foam was meshed using 8-node solid elements in the ELFORM_1 formulation [11, 12].

The screw connections between the guiderail segments were described by beam elements with stiffness properties (material model *MAT_68_NONLINEAR_PLASTIC_DISCRETE_BEAM [11, 12]), obtained on the basis of 3D modeling of bolted joints [14]. Remaining screw joints of the CFR2 overlay with the SP-05/2 system, were modelled with the use of *CONSTRAINED_GENERALIZED_ WELD_SPOT [11, 12], with respective load capacities resulting from the strength classes of the used screws [2].

*MAT_024_PIECEWISE_LIEAR_PLASTICITY material model was used for describing the S235JR material properties, which is an elastic-plastic model with isotropic hardening and failure criterion based on effective plastic strain, [11, 12]. The material constants were taken from the quality certificate for the Stalprodukt product [16, 18, 21].

The CFR2 overlay laminate was described by a linear-elastic-brittle material model *MAT_054_ENCHANCED_COMPOSITE_DAMAGE, with the Chang-Chang failure criterion [11, 12]. This model is mainly designed for unidirectional reinforced composites. However, as shown in Ref. [24], it can also be used for laminates reinforced with fabrics. Elasticity and strength constants of composite laminas were obtained based on experimental tests conducted in the Laboratory of Materials and Structures Strength of the Department of Mechanics and Applied Computer Science, Faculty of Mechanical Engineering of Military University of Technology, Warsaw [16, 18, 21]. Polyurethane foam was described by *MAT_026_HONEYCOMB material model [11, 12]. The material constants for PUR S-42 polyurethane foam were taken from Ref. [8].

Details of the modelling of the tested systems can be found in Refs. [16, 18, 21].

4. Base TB11 Virtual Crash Tests

The base TB11 virtual crash tests named the test for barriers in an arc of 150 m radius without an overlay (code TB11/CB/20) and with a CFR2 overlay (code TB11/CBC/20). The results for the base crash tests are shown in figs. 3 and 4. Figure 3 shows an example of unacceptable vehicle behaviour, which fishtailed and cross the front line of the exit box, [25, 26]. The TB11/CB/20 virtual crash test does not ensure the acceptance of an SP-05/2 barrier in an arc of 150 m radius. The use of a CFR2 overlay (Fig. 4) ensures the correct redirection of the vehicle.
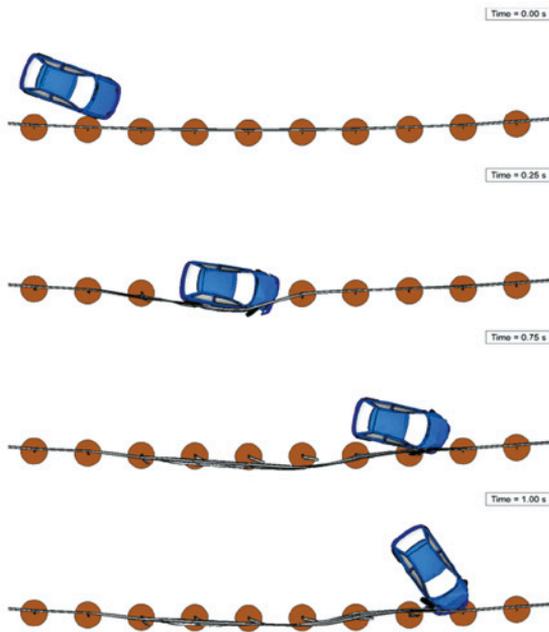
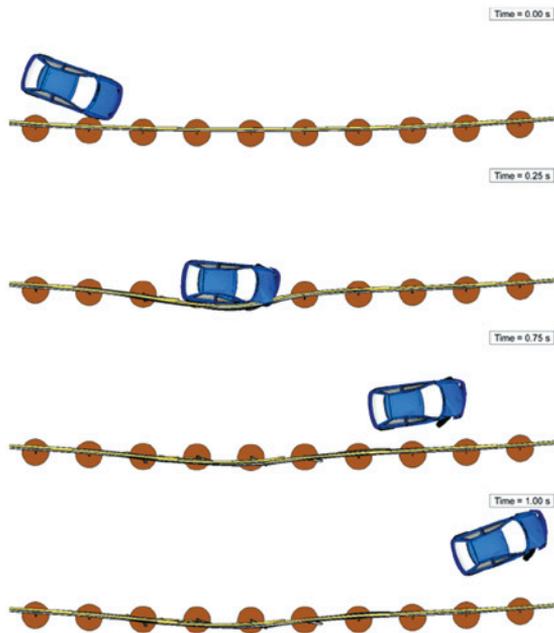Fig. 3. Simulation of TB11/CB/20 crash test– top view

Fig. 4. Simulation of TB11/CBC/20 crash test – top view

Figure 5 compares the energy balances for the tests. For the TB11/CB/20, as a result of the collision, 95% of the vehicle kinetic energy is absorbed, whereas the energy absorbed as a result of the material damage amounts to 0.195 MJ. For the TB11/CBC/20, as a result of the collision, 79% of the vehicle kinetic energy is absorbed, whereas the energy absorbed as a result of the material damage amounts to 0.161 MJ. The residual velocity of the vehicle at the end of the vehicle-barrier interaction amounts to 47.5 km/h.

Table 2 summarizes the results of the base virtual crash tests TB11/CB/20 and TB11/CBC/20. The influence of the CFR2 overlay on the course of the TB11 crash test for barriers in an arc is significant. In the first phase of the test (time below 0.45 s), there is a marginal reduction in the kinetic energy and a slight increase of the internal energy, as compared to the unmodified barrier (without CFR2 overlay). Later in the process, the kinetic energy and internal energy were maintained at a constant level (test TB11/CBC/20), which guarantees the approval of the crash test.

For both testing variants, the ASI and THIV parameters correspond to the level of impact intensity for the analyzed barrier (level A, [25, 26]). In the case of TB11/CBC/20 the working width is reduced by 15.3%. Simultaneously, the vehicle-barrier interaction length is reduced by 47.2%.
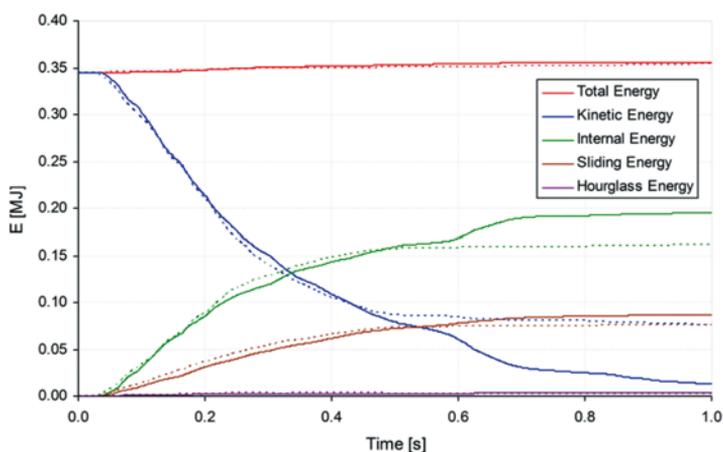

Fig. 5. Comparison of energy balances of TB11/CB/20 (solid lines) and TB11/CBC/20 (dashed lines) tests

5. Analyzed Parameters for TB11 Virtual Crash Test

On the road bends the vehicle impact angle with the barrier may be reduced or increased in relation to the standard-specific angle [25, 26]. Also the atmospheric conditions that influence the state of the road surface may change. To demonstrate the desirability of applying

the CFR2 overlay, the selected parameters of the setting were analyzed, based on the series of TB11 virtual crash tests. Table 1 summarizes the analyzed tests.

TB11/CB/20 and TB11/CBC/20 tests corresponds to a dry road and roadside surface, for which the coefficient of friction between the tires and the surface is 0.90, and between the tires and the shoulder is 0.68 [30]. For wet roads and shoulders, these coefficients respectively assume the values of 0.60 and 0.55 [30].

6. Influence of Impact Angle

The results for TB11/CB/10 crash test simulation are shown in fig. 6. During the collision, there are two impacts, the second of which is not taken into consideration, in accordance with Refs. [25, 26]. The damage and deformation of the vehicle is insignificant and affects exclusively the front wheelset. The results for TB11/CBC/10 crash test simulation are shown in fig. 7. In this case, there are also two collisions, and the result of the collision is also damage of the front wheelset exclusively.

Table 1. The tests covered by analysis of influence of selected parameters

| Setting/test code	Description of the setting	Aim of numerical calculations
TB11/CB/10 TB11/CB/30	vehicle/ground/barrier system, TB11 test, barrier in arc without overlay, impact angle of 10° and 30°	influence of impact angle
TB11/CBC/10 TB11/CBC/30	vehicle/ground/overlay/barrier system, TB11 test, barrier in arc with overlay, impact angle of 10° and 30°	influence of impact angle
TB11/CB/20_Wet	vehicle/ground/barrier system, modified TB11 test, barrier in arc without overlay, impact angle of 20°, wet road and shoulder surfaces	influence of wet road and shoulder surfaces
TB11/CBC/20_Wet	vehicle/ground/barrier system, modified TB11 test, barrier in arc without overlay, impact angle of 20°, wet road and shoulder surfaces	influence of wet road and shoulder surfaces

Time = 0.00 s

Time = 0.25 s

Time = 0.75 s

Time = 1.00 s
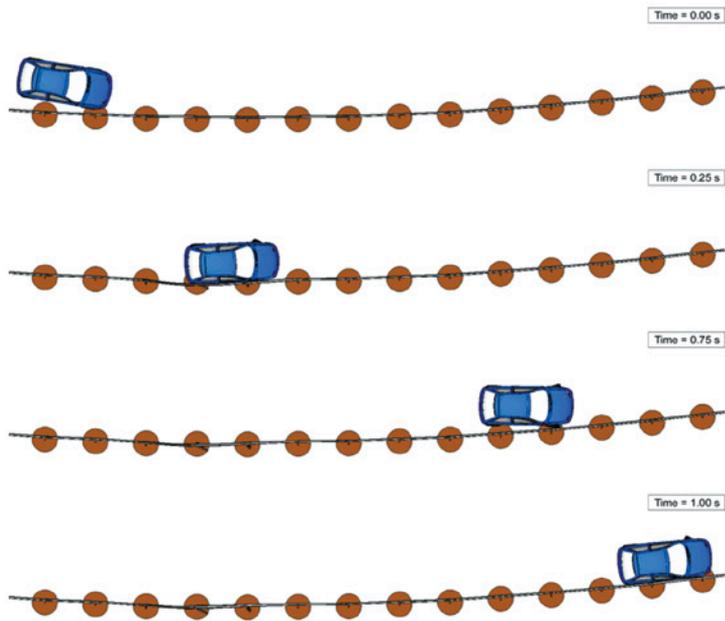
Fig. 6. Simulation of TB11/CB/10 crash test – top view

Time = 0.00 s

Time = 0.25 s
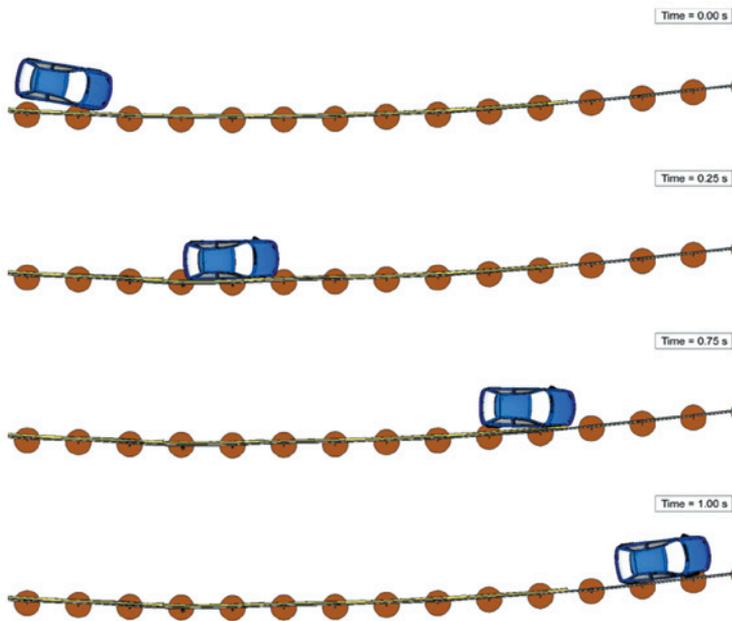
Time = 0.75 s

Time = 1.00 s

Fig. 7. Simulation of TB11/CBC/10 crash test – top view

Figure 8 compares the energy balances for the above tests. For the TB11/CB/10, as a result of the collision, 42.9% of the vehicle kinetic energy is absorbed, whereas the energy absorbed as a result of the material damage amounts to 0.067 MJ. The residual velocity of the vehicle at the end of the vehicle-barrier interaction amounts to 83.9 km/h.

For the TB11/CBC/10, as a result of the collision, 44.9% of the vehicle kinetic energy is absorbed, whereas the energy absorbed as a result of the material damage amounts to 0.070 MJ. The residual speed of the vehicle at the end of the vehicle-barrier interaction amounts to 84.6 km/h.
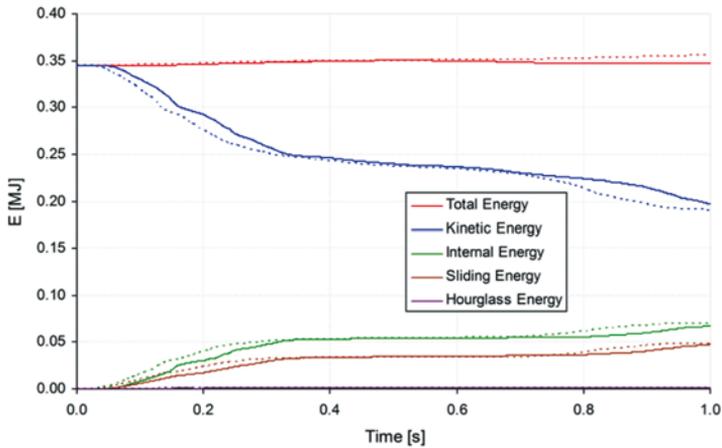

Fig. 8. Comparison of energy balances of TB11/CB/10 (solid lines) and TB11/CBC/10 (dashed lines) tests

Table 2 summarizes the results of the TB11/CB/10 and TB11/CBC/10 virtual crash tests. For the impact angle of 10° the influence of the overlay on the values of the majority of the functionality parameters and the impact phenomenon itself is insignificant. Only the vehicle-barrier interaction length underwent a significant change (reduced by 47.2%). In addition, introducing the overlay, results in an increase of 11.3% for ASI and of 3.7% for the working width and in a decrease of 5.9% for THIV and of 0.8% for the residual speed.

The results for TB11/CB/30 crash test simulation are shown in fig. 9. Figure 10 shows the crash test simulation results for TB11/CBC/30. In the case of the barrier without the overlay the vehicle penetrated the barrier and was blocked. The use of CFR2 overlay also resulted in the vehicle penetrating the barrier, and subsequently rebounding and fishtailing. In both cases, the damage to the vehicle is considerable. The integrity of the containment system is intact (despite considerable damage to the overlay in the case of TB11/CBC/30 test).
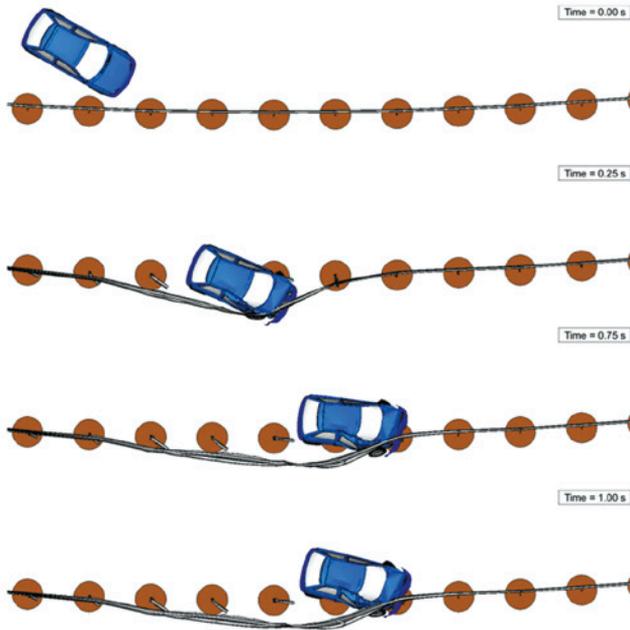
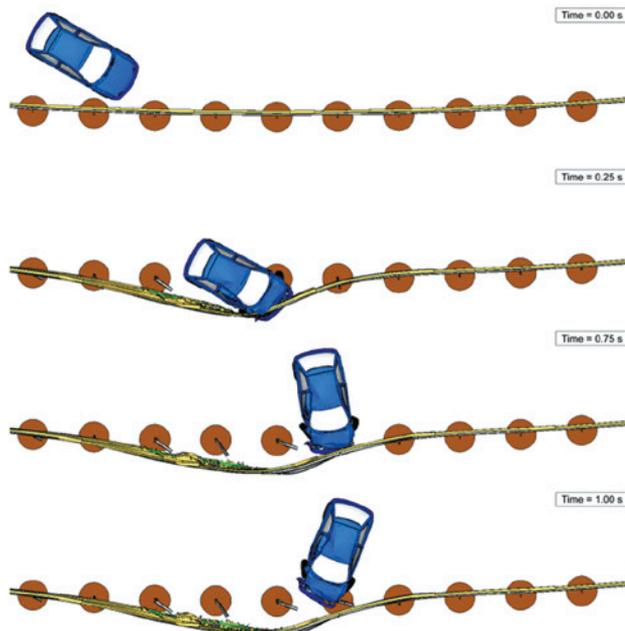Fig. 9. Simulation of TB11/CB/30 crash test – top view

Fig. 10. Simulation of TB11/CBC/30 crash test – top view

Figure 11 compares energy balances of the above tests. For the TB11/CB/30, as a result of the collision, 99% of the vehicle kinetic energy is absorbed, whereas the energy absorbed as a result of material damage amounts to 0.232 MJ. For the TB11/CBC/30, as a result of the collision, 98% of the vehicle kinetic energy is absorbed, whereas the energy absorbed as a result of material damage amounts to 0.251 MJ.
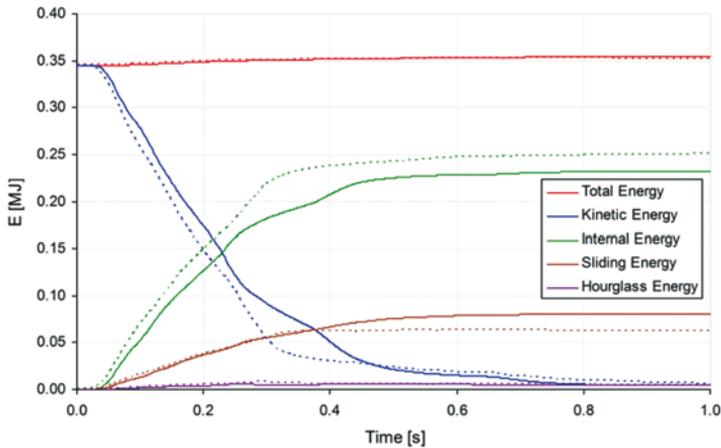

Fig. 11. Comparison of energy balances of TB11/CB/30 (solid lines) and TB11/CBC/30 (dashed lines) tests

Table 2 summarizes the results of the TB11/CB/30 and TB11/CBC/30 virtual crash tests. For the impact angle of 30° the used CFR2 overlays cause an increase of 19.2% for ASI and of 13.4% for THIV, as well as a decrease of the working width by 2% and a decrease of the vehicle-barrier interaction length by 27.1%. The use of CFR2 overlay results in increased rigidity of the barrier.

7. Influence of Wet Road and Shoulder Surfaces

The results for TB11/CB/20_Wet crash test simulation are shown in fig. 12. The vehicle is stopped by the barrier and subsequently fishtails. Damage to the vehicle is significant. The results for TB11/CB/20_Wet crash test simulation are shown in fig. 13. Redirection of the vehicle is correct. Damage to the vehicle is minor and mainly involves the front wheelset.

Virtual crash tests for the barrier in an arc without CFR2 overlay and with CFR2 overlay, under dry road and shoulder surface conditions consider the TB11/CB/20 and TB11/CBC/20 tests, respectively.
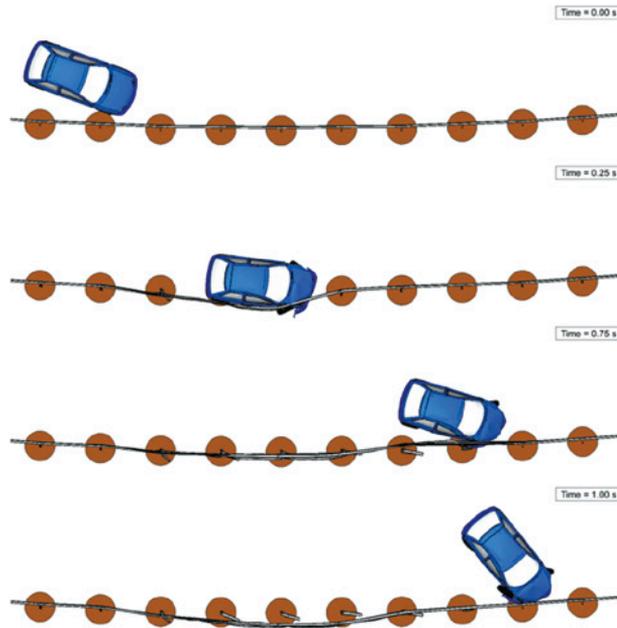
Time = 0.00 s

Time = 0.25 s

Time = 0.75 s

Time = 1.00 s

Fig. 12. Simulation of TB11/CB/20_Wet crash test – top view

Time = 0.00 s

Time = 0.25 s
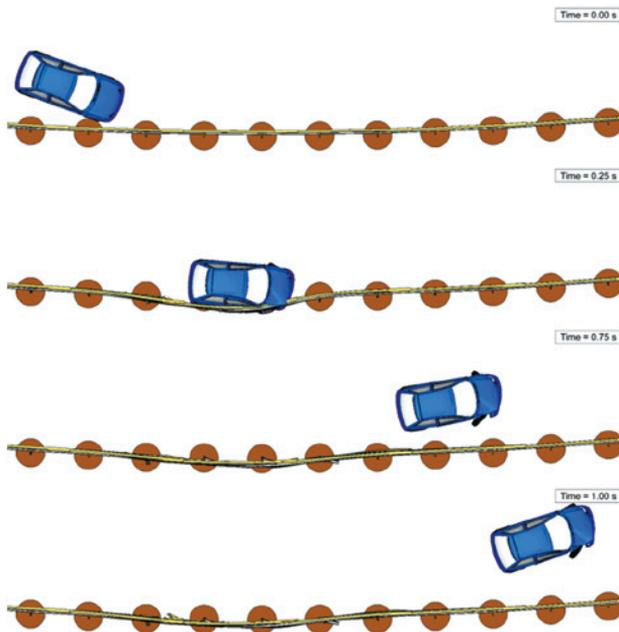
Time = 0.75 s

Time = 1.00 s

Fig. 13. Simulation of TB11/CBC/20_Wet crash test – top view

Table 2 summarizes the results of the TB11/CB/20_Wet and TB11/CBC/20_Wet virtual crash tests.

The comparison of the energy balances under dry road and shoulder surface conditions is shown in Fig. 5. Figure 14 compares the energy balances of TB11/CB/20_Wet and TB11/CBC/20_Wet tests. For the TB11/CB/20_Wet, as a result of the collision, 92.1% of the vehicle kinetic energy is absorbed, whereas the energy absorbed as a result of the material damage amounts to 0.199 MJ. For the TB11/CBC/20_Wet, as a result of the collision, 75.0% of the vehicle kinetic energy is absorbed, whereas the energy absorbed as a result of the material damage amounts to 0.163 MJ.

The crash tests without an overlay under both dry and wet conditions result in a failure to comply with the basic test acceptance criterion, which is the correct recovery of the vehicle through the barrier. Introducing a CFR2 overlay results in approval of the crash test, according to [3, 4]. The vehicle is correctly redirected from the interaction with the barrier, which is positively influenced by the 35% increase of residual speed in comparison to the conditions of dry road and roadside surface.
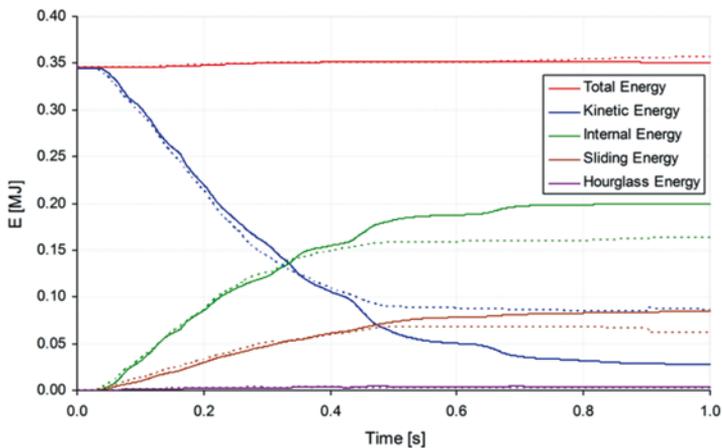

Fig. 14. Comparison of energy balances of TB11/CB/20_Wet (solid lines) and TB11/CBC/20_Wet (dashed lines) tests

Table 2. Comparison of results of the analyzed virtual crash test

Dynamic system	ASI	THIV [km/h]	VCDI	W [m]	$L^{2)}$ [m]	CBE[3]	$E^{4)}$ [MJ]	$v_r^{5)}$ [km/h]
TB11/CB/101)	0.62	12.62	RF0000000	0.27	5.05	yes	0.181	83.9
TB11/CB/201)	0.85	20.91	RF0010000	0.85	12.3	no	0.195	-
TB11/CB/20_Wet	0.87	17.20	RF0010000	0.80	12.1	no	0.199	-
TB11/CB/301)	0.78	23.29	RF1010001	1.51	8.50	no	0.232	-
TB11/CBC/101)	0.55	13.36	RF0000000	0.26	3.95	yes	0.154	84.6
TB11/CBC/201)	0.80	19.21	RF0010110	0.72	6.50	yes	0.161	47.5
TB11/CBC/20_Wet	0.78	16.71	RF0010100	0.77	5.95	yes	0.163	64.3
TB11/CBC/301)	0.93	26.40	RF1010001	1.48	6.20	no	0.251	-

[1] results for dry road and shoulder surface conditions

[2] vehicle-barrier interaction length

[3] correct behavior of the vehicle in the exit box

[4] energy absorbed as a result of material damage

[5] residual velocity

8. Conclusion

The paper discusses the influence of selected parameters, i.e. the vehicle impact angle and dry/wet surface of roads and roadsides on the process of a TB11 virtual crash test for a SP-05/2 barrier in a horizontal concave arc of a 150 m radius. For the standard-specific impact angle of 20°, in both dry and wet conditions, the use of CFR2 foam-composite overlay results in the approval of with the acceptance criteria for a TB11 crash test.

In addition, the TB11 virtual test on the influence of the vehicle impact angle with a SP-05/2 barrier in a horizontal concave arc of a radius of 150 m, of N2-W4-A class resulted in the following conclusions:

1) Increasing the vehicle-barrier impact angle in an arc without the overlay will result in an increase of ASI, THIV, VCDI, W, except for the ASI value for an angle of 30°. For impact angles of 10°, 20°, 30°, the ASI and THIV values meet the crash test acceptance conditions (ASI ≤ 1.0, THIV ≤ 33 km/h). The standard-specific value W4 ≤ 1.3 m for the working width is only exceeded for an angle of 30°.

2) Increasing the vehicle-barrier impact angle in an arc with the overlay results in an increase of ASI, THIV, VCDI, W parameters, except for the ASI value for an angle of 30°. For impact angles of 10°, 20°, 30°, the ASI and THIV values meet the crash test acceptance conditions (ASI ≤ 1.0, THIV ≤ 33 km/h). The standard value W4 ≤ 1.3 m for the working width is only exceeded for an angle of 30°.

3) For the impact angle of 10° the influence of the overlay on the values of the functionality parameters is insignificant. For the impact angle of 10° the overlay results in appropriate redirection of the vehicle onto the road, further resulting in the acceptance of TB11 test. In addition, a CFR2 overlay has significant influence on the lowering the

barrier guide in the impact zone, which eliminates the risk of the vehicle's cab being hit by the guiderail. For an angle of 30° the overlay reinforces the barrier, causing a significant increase in ASI and THIV parameters in comparison to an angle of 20°, respectively by 19% and 13%, and rebounds and fishtails the vehicle.

The TB11 virtual test on the influence of wet road and shoulder surfaces on the collision of a Geo Metro vehicle with a SP-05/2 barrier in the horizontal concave arc of a 150 m radius, of class N2-W4-A, resulted in the following conclusions:

1) Wet road and shoulder surface as compared to dry road and shoulder surface, had an insignificant effect on the TB11 test run with respect to the barriers without an overlay, in a horizontal concave arc of a radius of 150 m (Fig. 3 and Table 2). In wet conditions, as compared to the dry conditions, ASI is increased by approximately 2.4% and THIV by approximately 17.7%, the working width is increased by 5.9% and the vehicle-barrier interaction length is increased by 1.6%. The crash test cannot be accepted in neither case, dry or wet.

2) Wet road and shoulder surface, as compared to dry road and shoulder surface, resulted in the improvement of some parameters of the TB11 test with respect to the barriers with CFR2 overlay, in a horizontal concave arc of a radius of 150 m (Fig. 3 and Table 2). One of the main criteria for the acceptance of the crash test is a correct recovery of the vehicle onto the road, so any improvement of parameters that indirectly affect this ability is desirable (e.g. the vehicle-barrier interaction length, the residual speed, the VCDI). In the case of wet surface of roads and roadsides, as compared to dry conditions, the vehicle-barrier interaction length is reduced by 8.4% and the residual speed is significantly increased by 35%, which has a beneficial effect on recovering the vehicle onto the roadway. Moreover, the reduction of distance between the lower edge of the right panel and the upper edge of the left panel is ≤3% (for barrier without the overlay the change is greater, within the range of 3÷10%).

Acknowledgments

The full text of the article is available in Polish online on the website http://archiwummotoryzacji.pl.

Tekst artykułu w polskiej wersji językowej dostępny jest na stronie http://archiwummotoryzacji.pl.

References

[1] Atahan A O. Finite element simulation of a strong-post W-beam guardrail system. Simulation. 10 (2002); 78: 587-599.

[2] Biegus A. Połączenia śrubowe. Wydawnictwo Naukowe PWN. 1997; Warszawa-Wrocław.

[3] Borkowski W, Hryciów Z, Rybak P, WysockI J. Analiza skuteczności betonowych barier ochronnych na łuku drogi. Przegląd Mechaniczny. Rok LXXI, Z. 7-8/2012: 21–24

[4] Borkowski W, Hryciów Z, Rybak P, Wysocki J. Numerical simulation of the standard TB11 and TB32 tests for a concrete safety barrier. J. KONES Powertrain and Transport. 4 (2010); 17: 63–71.

[5] Borkowski W, Hryciów Z, Rybak P, Wysocki J. Testing the results of a passenger vehicle collision with a rigid barrier. J. KONES Powertrain and Transport. 1 (2010); 17: 51–57.

[6] Borovinsek M, Vesenjak M, Ulbin M, Ren Z. Simulating the impact of truck on road-safety barrier. Journal of Mechanical Engineering. (2006) 2; 52: 101–111.

[7] Borovinsek M, Vesenjak M, Ulbin M, Ren Z. Simulation of crash test for high containment levels of road safety barriers. Engineering Failure Analysis. 14 (2007): 1711-1718.

[8] Dziewulski P. Examination of Selected Structures to Improve Energy Intensity of Road Safety Barriers (in Polish). PhD Thesis, Military University of Technology. 2010; Warsaw.

[9] Dziewulski P. Numerical analysis of car – road barrier crash tests [in Polish]. Proc. III Symp. on Advances in Manufacturing Technologies and Machinery Structures, Kazimierz Dolny, Poland. 2009: 43-49.

[10] Goubel C, Di Pasquale E, Massenzio M, Ronel S. Comparison of crash tests and simu-lations for various vehicle restraint systems. 7th European LS-DYNA Conference. DYNAmore, GmbH, CD Proc. 2009: 1–12.

[11] Hallquist J O. LS-DYNA Keyword User's Manual. Livermore Sofware Technology Corporation, Livermore, CA, USA. May 2007.

[12] Hallquist J O. LS-DYNA Theory Manual. Livermore Sofware Technology Corporation, Livermore, CA, USA. March 2006.

[13] Kiczko A, Niezgoda T, Nowak J, Dziewulski, P. Numerical implementation of car impact into the modified road barrier. J. KONES Powertrain and Transport. 3 (2010); 17: 189-196.

[14] Klasztorny M, Kiczko A, Nycz D. Modelowanie numeryczne i symulacja rozciągania połączenia śrubowego segmentów prowadnicy B bariery drogowej. 13. Konf. Nauk.-Tech. Techniki Komputerowe w Inżynierii, Licheń Stary. 2014: 77-78.

[15] Klasztorny M, Niezgoda T, Romanowski R, Nycz D, Rudnik D, Zielonka K. Nakładka na prowadnicę bariery ochronnej na łuku drogi. Zgłoszenie patentowe UP RP. 6.10.2014.

[16] Klasztorny M, Nycz D B, Romanowski R K. Rubber/foam/composite overlay onto guide B of barrier located on road bend. The Archives of Automotive Engineering. 3 (2015); 69: 65-86.

[17] Klasztorny M, Romanowski R K, Nycz D B. Nakładka kompozytowo-pianowa na prowadnicę B drogowej bariery ochronnej w łuku poziomym wklęsłym – część 1: Projekt nakładki na prowadnicę bariery SP-05/2. Materiały kompozytowe. 3/2015: 36-38.

[18] Klasztorny M, Romanowski R K, Nycz D B. Nakładka kompozytowo-pianowa na prowadnicę B drogowej bariery ochronnej w łuku poziomym wklęsłym – część 2: Modelowanie i symulacja testów zderzeniowych. Materiały kompozytowe. 4/2015: 8-10.

[19] Nasution R P, Siregar R A, Fuad K, Adom A H. The effect of ASI (Acceleration Severity Index) to different crash velocities. Int. Conf. on Applications and Design in Mechanical Engineering (ICADME), CD Proc. 1–6. Malaysia. 11–13 October 2009.

[20] Niezgoda T, Barnat W, Dziewulski P, Kiczko A. Numerical modelling and simulation of road crash tests with the use of advanced CAD/CAE systems. Journal of KONBiN. 3 (2012); 23: 95-108.

[21] Nycz D. Modelowanie i badania numeryczne testów zderzeniowych bariery klasy N2-W4-A na łukach dróg. Wydawnictwo WAT. 2015; Warszawa.

[22] Ren Z, Vesenjak M. Computational and experimental crash analysis of the road safety barrier. Engineering Failure Analysis. 12 (2005): 963-973.

[23] Vesenjak M, Borovinšek M, Ren Z. Computational simulations of road safety barriers using LS-DYNA. 6. LS-DYNA Anwenderforum. DYNAmore, GmbH, Frankenthal, CD Proc. 2007: 1-8.

[24] Wade B, Feraboli P, Osborne M. Simulating laminated composites using LS-DYNA material model MAT54 part I: [0] and [90] playsingle-element investigation [cited 2014 Sep 22]. Available from: https://depts.washington.edu/amtas/events/jams_12/papers/paper-feraboli.pdf

[25] PN-EN 1317-1:2010. Systemy ograniczające drogę – część 1: Terminologia i ogólne kryteria metod badań.

[26] PN-EN 1317-2:2010. Systemy ograniczające drogę – część 2: Klasy działania, kryteria przyjęcia badań zderzeniowych i metody badań barier ochronnych i balustrad.

[27] Stalowe bariery ochronne. Stalprodukt S.A. 2006; Bochnia.

[28] System N2 W4 (SP-5/2). Stalprodukt S.A. 2011; Bochnia.

[29] Vehicle Models, NCAC, USA, January 7, 2013. Available from: http://www.ncac.gwu.edu/vml/models.html

[30] Tire friction and rolling resistance coefficients, Denmark, July 1, 2013. Available from:http://hpwizard.com/tire-friction-coefficient.html